Four decades of water quality change in the upper San Francisco Estuary

Marcus W. Beck[1*], Thomas W. Jabusch[2], Philip R. Trowbridge[2], David B. Senn[2]

[*] Corresponding author: marcusb@sccwrp.org

[1] *Southern California Coastal Water Research Project*
3535 Harbor Blvd, Suite 110, Costa Mesa, CA 92626

[2] *San Francisco Estuary Institute*
4911 Central Ave, Richmond, CA 94804

Declarations of interest: none

Version Date: Fri Feb 2 17:52:16 2018 -0800

Abstract

Quantitative descriptions of chemical, physical, and biological characteristics of estuaries are critical for developing an ecological understanding of drivers of change. Historical trends and relationships between key species of dissolved inorganic nitrogen (ammonium, nitrate/nitrite, total) from the Delta region of the San Francisco Estuary were modeled with an estuarine adaptation of the Weighted Regressions on Time, Discharge, and Season (WRTDS). Analysis of flow-normalized data revealed trends that were different from those in the observed time-series. Flow-normalized data exhibited changes in magnitude and even reversal of trends relative to the observed data. Modelled trends demonstrated that nutrient concentrations were on average higher in the last twenty years relative to the earlier periods of observation, although concentrations have been slowly declining since the mid-1990s and early 2000s. We further describe mechanisms of change with two case studies that evaluated 1) downstream changes in nitrogen following upgrades at a wastewater treatment plant, and 2) interactions between biological invaders, chlorophyll, macro-nutrients (nitrogen and silica), and flow in Suisun Bay. WRTDS results for ammonium trends showed a distinct signal as a result of upstream wastewater treatment plant upgrades, with specific reductions observed in the winter months during low-flow conditions. Results for Suisun Bay showed that chlorophyll *a* production in early years was directly stimulated by flow, whereas the relationship with flow in later years was indirect and influenced by grazing pressure. Although these trends and potential causes of change have been described in the literature, results from WRTDS provided an approach to test alternative hypotheses of spatiotemporal drivers of nutrient dynamics in the Delta.

Key words: estuary, nitrogen, Sacramento - San Joaquin Delta, trend analysis, weighted regression

1 Introduction

Understanding drivers of water quality change in estuaries depends on accurate descriptions of source inputs. The Sacramento - San Joaquin River Delta (hereafter 'Delta') is a mosaic of inflows in the upper San Francisco Estuary (SFE) that receives and processes nutrient inputs from primarily urban sources, in addition to agricultural sources (Jassby and Cloern 2000, Jassby et al. 2002, Jassby 2008). Although water quality conditions in the SFE symptomatic of eutrophication have historically been infrequent, recent responses to stressors suggests that ecosystem condition may be changing from past norms. Changes in phytoplankton biomass and composition, water clarity changes from sediment alteration, increases in harmful cyanobacterial blooms (*Microcystis aeruginosa*), increases in non-native macrophytes, and periodic events of low dissolved oxygen have been a recent concern for management of the Delta (Lehman et al. 2005, Santos et al. 2009, Hestir et al. 2013, Lehman et al. 2015, Dahm et al. 2016, ASC 2017). Although these changes are linked to drivers at different spatial and temporal scales, describing inputs from the Delta is critical to understand downstream effects.

Rates of primary production in coastal habitats are often defined by nutrient concentrations, although a simple relationship between enrichment and water quality changes can be difficult to determine (Cloern 2001). Nutrient concentrations are generally non-limiting for phytoplankton growth in the upper SFE, whereas light availability is the primary limiting factor preventing accumulation of phytoplankton biomass (Cole and

Cloern 1984, Alpine and Cloern 1988). Grazing pressure from pelagic fishes and benthic invertebrates can also reduce phytoplankton during periods of growth (Nichols 1985, Jassby 2008, Kimmerer and Thompson 2014). Moreover, changes in flow management practices compounded with climate variation have altered flushing rates and turbidity as key factors that moderate phytoplankton growth in the system (Alpine and Cloern 1992, Lehman 2000, Wright and Schoellhamer 2004, Canuel et al. 2009). Glibert et al. (2014) attributed recent phytoplankton blooms in Suisun Bay to a drought, during which residence times and nitrification rates increased. Speciation changes in the dominant forms of nitrogen confound a direct interpretation of links with phytoplankton blooms and the relationships between nutrients and primary production in the upper estuary are not completely understood. Although phytoplankton concentrations have been relatively consistent in recent years in Suisun Bay, biomass trends in the Delta are mixed (Jassby 2008, ASC 2017). Descriptions of nitrogen trends over several decades could be used to better understand long-term and more recent changes, particularly in the context of primary production and physical drivers of change (Dahm et al. 2016).

Long-term monitoring data are powerful sources of information that can facilitate descriptions of water quality change. A comprehensive water quality monitoring program has been in place in the upper SFE for several decades (Fig. 1, IEP 2013). Although these data have been used extensively (e.g., Lehman 1992, Jassby 2008, Glibert 2010), water quality trends covering the full spatial and temporal coverage of the Delta have not been systematically evaluated. Quantitative descriptions of nutrient dynamics are challenging given multiple sources and the volume of water that is exchanged with natural and anthropogenic processes. An evaluation using mass-balance models to describe nutrient

dynamics in the Delta demonstrated that the majority of ammonium entering the system during the summer is nitrified or assimilated, whereas a considerable percentage of total nitrogen load to the Delta is exported (Novick et al. 2015). Seasonal and annual changes in the delivery of water inflows and water exports directly from the system can also obscure trends (Jassby and Cloern 2000, Jassby 2008). It is important to consider these variable effects to characterize different trends in nitrogen forms.

Formal methods for trend analysis are required to describe water quality changes that vary by space and time. As a practical approach for water quality evaluation, trend analysis of ecosystem response indicators often focuses on tracking the change in concentrations or loads of nutrients over many years. Response indicators can vary naturally with changing flow conditions and may also reflect long-term effects of management or policy changes. Similarly, nutrient trends that vary with hydrologic loading can vary as a function of utilization rates by primary producers or decomposition processes (Sakamoto and Tanaka 1989, Schultz and Urban 2008, Harding et al. 2016). Concentration of chlorophyll *a* (chl-*a*) as a measure of phytoplankton response to nutrient inputs can follow seasonal patterns with cyclical variation in temperature and light changes throughout each year, whereas annual trends can follow long-term variation in nutrient inputs to the system (Cloern 1996, Cloern and Jassby 2010). Describing the relationship of a water quality variable as changing (chemodynamic) or invariant (chemostatic) with flow can isolate components, such as nutrient inputs, for a more direct assessment of causal factors (Wan et al. 2017).

The Weighted Regressions on Time, Discharge, and Season (WRTDS) approach was developed in this context and has been used to characterize decadal trends in river systems

(Hirsch et al. 2010, Sprague et al. 2011, Medalie et al. 2012, Hirsch and De Cicco 2014, Pellerin et al. 2014, Zhang et al. 2016). The WRTDS method has been adapted for trend analysis in tidal waters, with a focus on chl-*a* trends in Tampa Bay (Beck and Hagy III 2015) and the Patuxent River Estuary (Beck and Murphy 2017). Although the WRTDS method has been effectively applied to describe changes in freshwater systems, use in tidally influenced systems has not been as extensive. Application of WRTDS to describe trends in estuaries could reveal new insights given the disproportionate effects of physical drivers, such as flow inputs and tidal exchange, on water quality. The effects of biological drivers may also be more apparent because hydrological effects can be removed by WRTDS. As such, application of WRTDS models for trend analysis could facilitate a broader discusion on the need to focus beyond nutrients to develop integrated plans for water quality management.

The goal of this study was to provide a comprehensive description of nutrient trends in the Delta and Suisun Bay over the last forty years. This information can inform the understanding of ecosystem response dynamics and potential causes of water quality change. The specific objectives were to 1) quantify and interpret trends over four decades at ten stations in the Delta and Suisun Bay, including annual, seasonal, and spatial changes in nitrogen forms and response to flow variation, and 2) provide detailed descriptions of two case studies in the context of conceptual relationships modeled with WRTDS. The second objective evaluated two specific water quality stations to demonstrate complexities with nutrient response to flow, effects of nutrient-related source controls on ambient conditions, and effects of biological invasion by benthic filter feeders on nutrient cycling and primary production. Our general hypothesis was that the results were

expected to support previous descriptions of trends in this well-studied system, but that new insight into spatial and temporal variation in response endpoints was expected, particularly in flow-normalized model predictions.

2 Materials and Methods

2.1 Study system

The Delta region drains a 200 thousand km^2 watershed into the SFE, which is the largest estuary on the Pacific coast of North America. The watershed provides water to over 25 million people and irrigation for 18 thousand km^2 of agricultural land. Water enters the SFE through the Sacramento and San Joaquin rivers that have a combined inflow of approximately 28 km^3 per year, with the Sacramento accounting for 84% of inflow to the Delta. The SFE system includes the Delta and subembayments of San Francisco Bay (Fig. 1). Water dynamics in the SFE and Delta are governed by inflows from the watershed, tidal exchange with the Pacific Ocean, and water withdrawals for municipal and agricultural use (Jassby and Cloern 2000). Seasonally, inflows from the watershed peak in the spring and early summer from snowmelt, whereas consumption, withdrawals, and export have steadily increased from 1960 to present, but vary depending on inter-annual climate effects (Cloern and Jassby 2012). Notable drought periods have occurred from 1976-1977, 1987-1992, and recently from 2013-2015 (Cloern 2015).

Orthophosphate (PO_4^{3-}) and dissolved inorganic nitrogen (DIN) enter the Delta primarily through the Sacramento and San Joaquin rivers and from municipal wastewater treatment plant (WWTP) inputs. Annual nutrient export from the Delta region has been estimated as approximately 30 thousand kg d^{-1} of total nitrogen (varying with flow,

Novick et al. 2015), with 90% of ammonium (NH_4^+) originating solely from the Sacramento Regional WWTP (Jassby 2008). Although nitrogen and phosphorus inputs are considerable, primary production is relatively low and not nutrient-limited (Jassby et al. 2002, Kimmerer et al. 2012).

2.2 Data sources

Nutrient time series of monthly observations from 1976 to 2013 were obtained for ten active sampling stations in the Delta (Fig. 1 and Table 1, IEP 2013). Stations were grouped by location in the study area for comparison: *peripheral* Delta stations C3 (Sacramento inflow), C10 (San Joaquin inflow), MD10, and P8; *interior* Delta stations D19, D26, and D28; and *Suisun* stations D4, D6, and D7. These stations cover all of the major inflows and outflows to the Delta and were selected for analysis based on the continuity of the period of observation (Jabusch and Gilbreath 2009). Although many other stations are available for the region, the stations were chosen because they represent a consistent long-term dataset generated by a single program and they capture dominant seasonal and annual modes of nitrogen variability characteristic of the region (Jabusch et al. 2016). Time series were complete for all stations except for an approximate ten year gap from 1996-2004 for D19. Data were minimally processed, with the exception of averaging replicates that occurred on the same day. The three nitrogen forms that were evaluated were ammonium, nitrite/nitrate, and DIN (as the sum of the former two). Less than 3% of all observations were below the detection limit (left-censored), although variation was observed between nitrogen forms and location. The ammonium time series had the most censored observations at sites C10 (25.4% of all observations), MD10

(18.1%), D28 (17.8%), D19 (12%), and D7 (7.9%).

WRTDS models require flow data paired with nutrient data. At the Delta stations, daily flow estimates were matched with the corresponding sample dates for the nutrient data. Daily flow estimates were obtained from the Dayflow software program (IEP 2016). The Sacramento daily flow time series was used to account for flow effects at C3, D19, D26, D28, and MD10, and the San Joaquin time series was used for C10 and P8 based on station proximity to each inflow. Given the complexity of inflows and connectivity of the system, only the inflow estimates from the Sacramento and San Joaquin rivers were used as measures of freshwater influence at each station. Initial analyses indicated that model fit was not significantly improved with flow estimates from locations closer to each station, nor was model fit improved using lagged times series. Salinity was used as a proxy for flow at the Suisun Bay sites D4, D6, and D7 where tidal influences were much stronger. Salinity has been used as a tracer of freshwater influence for the application of WRTDS models in tidal waters (Beck and Hagy III 2015). Models were evaluated using salinity at the Delta stations, but performance was reduced relative to models that used daily flow estimates.

2.3 Analysis method and application

A total of thirty WRTDS models were created, one for each nitrogen form at each station. The functional form of WRTDS is a simple regression (Hirsch et al. 2010) that models the log-transformed response variable as a function of time, flow, and season:

$$\ln(N) = \beta_0 + \beta_1 t + \beta_2 \ln(Q) + \beta_3 \sin(2\pi t) + \beta_4 \cos(2\pi t) \quad (1)$$

where N is one of three nitrogen forms, time t is a continuous variable as decimal time to

capture the annual (β_1) or seasonal (β_3, β_4) trend, and Q is the flow variable (either flow or salinity depending on station).

The WRTDS model is a moving window regression that fits unique parameters (i.e., $\beta_0, \ldots, \beta_4$) at each observation point in the time series (n ranging from 433 at D19 to 571 at C3). Rather than fitting a global model to the entire time series, one regression is fit to every observation. Observations within a window for each regression are weighted relative to annual, seasonal, and flow distances from the observation at the center of the window. Observations with distances farther from the center (i.e., greater time and different flow values from the center) have less weight during parameter estimation for each regression. This approach allows for a type of smoothing where the observed fit is specific to the data characteristics within windows. Models applied herein were based on a tidal adaptation of the original method that can use either flow or salinity estimates as nutrient predictors (Beck and Hagy III 2015). All models were fit to describe the conditional mean response using a weighted Tobit model for left-censored data below the detection limit (Tobin 1958). Model predictions were evaluated as monthly values or as annual values that averaged monthly results within each water year (October to September). All analyses used the WRTDStidal package for the R statistical programming language (Beck 2017, RDCT (R Development Core Team) 2017). The default model fitting procedures were used that set half-window widths as six months for seasonal weights, ten years for annual weights, and half the range of salinity or flow in the input data for Q weights.

A hallmark of the WRTDS approach is the description of flow-normalized trends that are independent of variation from freshwater inflows (Hirsch et al. 2010) or tidal variation (Beck and Hagy III 2015). Flow-normalized trends for each analyte at each

station were used to describe long-term changes in different annual and seasonal periods. Flow-normalization predictions for each month of each year were based on the average of predictions for flow values that occur in the same month across all years, weighted within each specific month and year for every observation. Flow-normalized trends in each analyte were summarized as both medians and percent changes from the beginning to end of annual groupings from 1976-1995 and 1996-2013, and seasonal groupings of March-April-May (spring), June-July-August (summer), September-October-November (fall), and December-January-February (winter) within each annual grouping. Annual groupings were chosen as approximate twenty year midpoints in the time series and seasonal groupings were chosen to evaluate inter-annual changes while keeping season constant.

Trends in each annual and seasonal grouping were based on seasonal Kendall tests of the flow-normalized predictions. This test is a modification of the non-parametric Kendall test that accounts for variation across seasons in the response variable (Hirsch et al. 1982, Millard 2013). Results from the test can be used to evaluate the direction, magnitude, and significance of a monotonic change within the period of observation. The estimated rate of change per year is also returned as the Theil-Sen slope and was interpreted as the percent change per year when divided by the median value of the response variable in the period of observation (Jassby 2008). Trends in annual groupings were based on all monthly observations within relevant years, whereas seasonal groupings were based only on the relevant months across years. Seasonal Kendall tests were also used to describe trends in the observed data. These trends were compared with those based on the flow-normalized trends to evaluate potential differences in conclusions caused by flow effects.

2.4 Selected examples

Two stations were chosen to demonstrate use of WRTDS to develop a more comprehensive description of decadal trends in the Delta. The selected case studies focused on 1) effects of wastewater treatment upgrades upstream of P8, and 2) effects of biological invasion on nutrient dynamics in Suisun Bay using observations from D7. Each case study is built around hypotheses that results from WRTDS models were expected to support, both as a general description and for additional testing with alternative methods.

2.4.1 Effects of wastewater treatment

Significant efforts have been made in recent years to reduce nitrogen loading from regional WWTPs given the disproportionate contribution of nutrients relative to other sources (Cornwell et al. 2014, Novick et al. 2015). Several WWTPs in the Delta have recently been or are planned to be upgraded to include tertiary filtration and nitrification to convert biologically available ammonium to nitrate. The City of Stockton WWTP was upgraded in 2006 and is immediately upstream of station P8 (Jabusch et al. 2016), which provides a valuable opportunity to assess how nutrient or nutrient-related source controls and water management actions have changed ambient concentrations downstream. A decrease of ammonium concentrations at P8 after 2006 is expected as a result of upstream WWTP upgrades, and water quality should exhibit 1) a shift in the ratio of the components of DIN from the WWTP before/after upgrade, and 2) a flow-normalized annual trend at P8 to show a change concurrent with WWTP upgrades.

2.4.2 Effects of biological invasions

Invasion of the upper SFE by the Asian clam *Potamocorbula amurensis* in 1986 caused severe changes in phytoplankton abundance and species composition. Reduction in phytoplankton biomass has altered trophic networks in the upper SFE and is considered an important mechanism in the decline of the protected delta smelt (*Hypomesus transpacificus*) and other important fisheries (Feyrer et al. 2003, Mac Nally et al. 2010). Changes in the physical environment have also occurred, particularly increased water clarity from a reduction of particle transport and erodible sediment supply (Jassby 2008, Schoellhamer 2011, Cloern and Jassby 2012), although decreases in phytoplankton by clam biofiltration may have also increased clarity (Mac Nally et al. 2010). The clams are halophilic such that drought years are correlated with an increase in biomass and further upstream invasion of the species (Parchaso and Thompson 2002, Cloern and Jassby 2012). We hypothesized that results from WRTDS models would show 1) a decline in annual, flow-normalized chlorophyll concentrations over time coincident with an increase in abundance of invaders, and 2) variation in the chlorophyll/clam relationship through indirect or direct controls of flow. Although the relationship between phytoplankton and clams in the upper SFE has been well described (Kimmerer and Thompson 2014), we use WRTDS to develop additional evidence that an increase in DIN was facilitated in part by clam invasion and the relationship of phytoplankton with clam abundance was mediated by flow and climatic variation in recent years.

3 Results

3.1 Observed data and modelled trends

The observed time series for the ten Delta - Suisun Bay stations had substantial variation in scale among the nitrogen forms and differences in apparent seasonal trends (Fig. 2). DIN for most stations was dominated by nitrite/nitrate, whereas ammonium was a smaller percentage of the total. However, C3 had a majority of DIN composed of ammonium and other stations (e.g., P8, D26) had higher concentrations of ammonium during winter months when assimilation rates are lower (Novick et al. 2015). By location, observed concentrations of DIN for the entire time series were higher on average for the peripheral Delta stations (C3, C10, MD10, P8; mean ± s.e.: 1.04±0.03 mg L^{-1}) and similar for the interior Delta (D19, D26, D28, 0.43±0.01) and Suisun Bay stations (D4, D6, D7, 0.44±0.01). Average concentrations were highest at P8 (1.63±0.05 mg L^{-1}) and lowest at C3 (0.4±0.01) for DIN, highest at P8 (0.28±0.02) and lowest at D28 (0.05±0.003) for ammonium, and highest at C10 (1.4±0.04) and lowest at C3 (0.15±0.004) for nitrite/nitrate. Mean observed concentrations were also higher later in the time series for all forms. For example, average DIN across all stations was 0.61±0.01 mg $L^{-1}$for 1976-1995, compared to 0.7±0.01 for 1996-2013. Seasonal changes across all years showed that nitrogen concentrations were generally lower in the summer and higher in the winter, although observed patterns were inconsistent between sites. For example, site MD10 had distinct seasonal spikes for elevated DIN in the winter, whereas other stations had less prominent seasonal maxima (e.g., C3, D7, Fig. 2).

Relative to the observed data, long-term trends between stations for the different nitrogen forms were apparent from the modelled results (Fig. 3). Although each station varied in the overall concentrations, patterns within the three regions (peripheral Delta, interior Delta, and Suisun Bay) were observed. Concentrations for all nitrogen forms were highest in the peripheral stations. Ammonium concentrations were highest at P8 and C3 and showed a consistent increase over time, followed by a reduction beginning in the early 2000s, whereas ammonium concentrations at C10 and MD10 were low and gradually decreasing throughout the period of record. By contrast, DIN and nitrite/nitrate concentrations at the peripheral Delta stations showed increases at P8 and C10 followed by a decline in the early 2000s, whereas concentrations at C3 and MD10 were lower and did not show any noticeable trends. Trends at the interior Delta stations showed a gradual increase in ammonium followed by a gradual decrease beginning in the early 1990s, particularly for D26. Trends in DIN and nitrite/nitrate for the interior Delta stations showed a reduction early in the time series, followed by a slight increase beginning in the mid-1980s, and finally a reduction beginning in the late 1990s. These trends were similar for the Suisun Bay stations, although the reduction in the late 1990s did not occur. By contrast, ammonium concentrations were low in Suisun Bay but a gradual increase over the period of record was observed.

3.2 Trend tests

Estimated trends from Seasonal Kendall tests on the raw time series varied considerably between sites and nitrogen forms (Fig. 4). Significant trends were observed from 1976-1995 for eight of ten sites for DIN (seven increasing, one decreasing), eight sites

for ammonium (six increasing, two decreasing), and six sites for nitrite/nitrate (five increasing, one decreasing). Decreasing trends were more common for the observed data from 1996-2013. Eight sites had significant trends for DIN (four increasing, four decreasing), seven sites for ammonium (five increasing, two decreasing), and eight sites for nitrite/nitrate (four increasing, four decreasing). P8 had a relatively large decrease in ammonium (-8.3% change per year) for the second annual period compared to all other sites. Trends by season were similar such that increases were generally observed in all seasons from 1976-1995 (Fig. S1) and decreases were observed for 1996-2013 (Fig. S2). Trends for the seasonal comparisons were noisier and significant changes were less common compared to the annual comparisons.

A comparison of flow-normalized results from WRTDS relative to observed data identified changes in the magnitude, significance, and direction of trends. For all sixty trend comparisons in Fig. 4 (flow-normalized values in Table 2) regardless of site, nitrogen analyte, and time period (annual or seasonal aggregations), thirteen comparisons had trends that were insignificant ($p > 0.05$) with the observed data but significant with flow-normalized results, whereas only one trend changed to insignificant. This suggests that time series that include flow effects had sufficient noise to obscure or prevent identification of an actual trend of a water quality parameter. Further, changes in the magnitude of the estimated percent change per year were also apparent for the flow-normalized trends, such that fourteen comparisons showed an increase in magnitude (more negative or more positive) and twenty five had a decrease (less positive or less negative) compared to observed trends. Eleven comparisons showed a trend reversal from positive to negative estimated change, nine sites went from no change to negative estimated change, and one

site went from no change to a positive trend for the flow-normalized results. Differences by season in the observed relative to flow-normalized trends from WRTDS were also apparent (Figs. S1 and S2 and Tables S1 and S2). The most notable change in the flow-normalized results was an overall decrease (less positive trend or greater negative trend) in concentrations for most sites in the summer and fall seasons for 1996-2013. More statistically significant trends were also observed with the flow-normalized results.

3.3 Selected examples

3.3.1 Effects of wastewater treatment

Effluent measured from 2003 to 2009 from the Stockton WWTP had similar DIN concentrations before and after upgrades, whereas ammonium concentrations were greatly reduced (Fig. 5). Ammonium and nitrate concentrations were comparable prior to 2006, whereas nitrate was a majority of total nitrogen after the upgrade, with much smaller percentages from ammonium and nitrite. As expected, flow-normalized nitrogen trends at P8 shifted in response to upstream WWTP upgrades (Fig. 6a), with ammonium showing an increase from 1976 followed by a large reduction in the 2000s. Nitrite/nitrate concentrations at P8 also showed a similar but less dramatic decrease despite an increase in the WWTP effluent concentrations following the upgrade (Fig. 5). Percent changes from seasonal Kendall tests on flow-normalized results (Table 3) showed that both nitrogen species increased prior to WWTP upgrades (2% per year for nitrite/nitrate, 2.8% for ammonium), followed by decreases after upgrades (-1.9% for nitrite/nitrate, -16.6% for ammonium). Seasonally, increases prior to upgrades were highest in the summer for nitrite/nitrate (2.4%) and in the fall for ammonium (4.9%). Similarly, seasonal reductions

post-upgrade were largest in the summer for nitrite/nitrate (−4.3%) and largest for ammonium in the winter (−26.7%).

Nitrogen concentrations varied with flow, although relationships depended on season and year. Relationships of nitrite/nitrate with flow described by WRTDS showed flushing or dilution at higher flow (Fig. 6b). Seasonal variation was even more apparent for ammonium, although both nitrite/nitrate and ammonium typically had the highest concentrations at low flow in the winter (January). Additionally, strength of the flow/nutrient relationship changed between years. Nitrite/nitrate typically had the strongest relationship with flow later in the time series (i.e., larger negative slope), whereas ammonium had the strongest relationship with flow around 2000 in January.

3.3.2 Effects of biological invasions

Invasion in the 1980s showed a clear reduction of *Corbicula fluminea* and increase of *P. amurensis* (Fig. 7a), where biomass of the latter was negatively associated with flow from the Sacramento river (Fig. 7b). The increase in clam abundance was associated with a notable decrease in annually-averaged chl-*a* from WRTDS results (Fig. 7c), as expected if WRTDS is adequately capturing flow variation and identifying the well-established phytoplankton decrease beginning in the 1980s. A seasonal shift in the flow-normalized results was also observed such that chl-*a* concentrations were generally highest in July/August prior to invasion, whereas a spring maximum in April was more common in recent years (Fig. 7f). An increase in annually-averaged silicon dioxide (Fig. 7d) was coincident with the chl-*a* decrease, with the largest increases occuring in August (Fig. 7g). Further, DIN trends were similar to silicon-dioxide in both annual and seasonal changes (i.e., Figures 7e and 7h compared to 7d and 7g), such that an increase in both nutrients

earlier in the time series corresponded with the decrease in chl-*a*.

The relationship of chl-*a* with clam biomass was significant (Fig. 7i), with lower chl-*a* associated with higher biomass. However, the effect of flow on both clams and phytoplankton as a top-down or bottom-up control changed throughout the time series. The chl-*a*/flow relationship showed that increasing flow (decreasing salinity) was associated with a slight increase in chl-*a* followed by a decrease early in the time series (Fig. 7j), whereas overall chl-*a* was lower but a positive association with flow (negative with salinity) was observed later in the time series. Following clam invasion, chl-*a* concentrations were reduced by grazing but showed a positive and monotonic relationship with increasing flow. The increase in clam abundance was concurrent with decline in chl-*a* concentration, although variation in abundance between years was also observed. Clam abundance was reduced during high flow years in the late 1990s, 2006, and 2011 (7a). In the same years, WRTDS predictions for chl-*a* were higher than the flow-normalized component (Fig. 7c), which further suggests a link between increased flow and phytoplankton production.

4 Discussion

Water quality conditions in the Delta-Suisun Bay region are dynamic and not easily characterized from observed time series. Annual aggregations of WRTDS modelled results and application of formal trend analyses provided insight into the spatial and temporal variation of nitrogen forms in three distinct regions that is not possible with raw observations. A general conclusion is that nitrogen concentrations have showed a consistent decrease beginning in the mid-1990s and early 2000s, although average concentrations remain above those observed earlier in the period of record. These results are confirmed

visually from WRTDS (Fig. 3) and through significant results from trend tests (Fig. 4, Table 2). Although the overall trends suggest a system-wide reduction, considerable differences by location and analyte were characterized by the analysis and are important independent of overall trends. Nutrient concentrations were highest at peripheral Delta stations (C3, MD10, P8, and C10) that monitor inflows from the Sacramento and San Joaquin rivers. The highest concentrations among all nitrogen forms, ammonium in particular, were observed at P8 in the early 2000s as a direct consequence of WWTP inputs upstream prior to infrastructure upgrades. Elevated ammonium concentrations were also observed at C3 as a measure of upstream contributions from the Sacramento WWTP. By contrast, nitrite/nitrate concentrations were highest at C10 as a measure of contributions from the San Joaquin River to the south that drains a predominantly agricultural watershed.

Differing magnitudes of nitrogen forms between stations as a function of source type can have an effect on the relationship between flow and nutrients. Both Hirsch et al. (2010) and Beck and Hagy III (2015) used WRTDS results to demonstrate variation between flow and nutrient dynamics depending on pollutant sources. In particular, a chemodynamic (i.e., changing) response of nutrients with flow variation is common if nutrients originate primarily from the watershed through diffuse sources (Thompson et al. 2011, Wan et al. 2017). Increased flow may induce a change in nutrient concentrations, such that reduction may occur with flushing or an increase may occur through mobilization. By contrast, nutrient loads are relatively chemostatic or invariant with changes in flow if point-sources are the dominant contributor. These relationships are modelled particularly well with WRTDS, which can provide a means of hypothesizing unknown sources or verifying trends

in response to management actions. As noted above, C10 at the inflow of the San Joaquin River is dominated by nitrite/nitrate consistent with diffuse, agricultural inputs from the watershed. A logical expectation is that trends from observed data may vary considerably from trends with modelled results that are flow-normalized. Accordingly, trend analysis of nitrate/nitrate by year and season showed that percent changes at C10 were typically underestimated with the observed data during the recent period from 1996-2013 (Tables 2 and S2). This is consistent with an expected effect of flow on raw time series, particularly for chemodynamic behavior at locations that drain highly altered watersheds (Wan et al. 2017).

Our results underscore the importance of considering flow effects in the evaluation of water quality trends. There were important differences in trends between observed and flow-normalized data. These differences ranged from a simple change in the magnitude and significance of a trend, to more problematic changes where the flow-normalized trend could demonstrate a complete reversal relative to the observed (e.g., DIN trends for all Suisun stations from 1996-2013, Fig. 4). Differences in apparent trends underscore the importance of considering flow effects in the interpretation of environmental changes, particularly if trend evaluation is used to assess the effects of nutrients on ecosystem health or the effectiveness of past nutrient management actions. An alternative evaluation of flow in the Delta demonstrated that flow contributions from different sources vary considerably over time at each station (Novick et al. 2015). For example, flow at MD10 represents seasonally changing inputs from the Sacramento and San Joaquin rivers and other sources. For simplicity, our analysis considered only the dominant water source and used the total daily inflow estimates from either the Sacramento River or the San Joaquin River at any of the

Delta sites. Given that substantial differences with flow-normalized results were apparent from relatively coarse estimates of flow contributions, more precise differences could be obtained by considering the influence of multiple flow components at each location. Output from the Dayflow software program (IEP 2016) provides a complete mass balance of flow in the Delta that could be used to develop a more comprehensive description. Our analysis is the first attempt to model nutrient dynamics related to flow in the entire Delta, such that additional work should focus on improving the characterization of flow signals at each station.

Long-term trends in nutrient and phytoplankton concentations in Suisun Bay have also been the focus of intense study for many years (Cloern et al. 1983, Lehman 1992, Dugdale et al. 2007, Jassby 2008, Glibert et al. 2014). Our results demonstrated an overall increase in ammonium from the late 1970s to 2000, with initial flow-normalized values of annual averages estimated as approximately 0.05 mg L^{-}1 for the Suisun stations in 1976 to a maximum ranging from 0.08 mg L^{-1} (station D4) to above 0.1 mg L^{-1} (D6) in 2000 (Fig. 3). Trends from 1996-2005 evaluated in (Jassby 2008) showed a similar increase in ammonium. However, a reversal of trends in recent years may also be occuring in Suisun Bay, as model estimates suggest either relatively constant concentrations or even a decrease at some stations beginning around 2000 (e.g., D6, D7, Fig. 4). Combined with the shift towards a dominant spring peak in chloropyll growth (Fig. 7f), changing nitrogen ratios continue to be a concern for the management of production in the upper SFE.

4.1 Interpretation of case studies

Seasonal timings of water quality improvements and the link to flow changes are difficult to characterize from the observed time series. WRTDS models were used to characterize these changes at P8 and to develop additional hypotheses of factors that influence nutrient concentrations. A general conclusion is that ammonium reductions were concurrent with WWTP upgrades, but the reduction was most apparent at low-flow in January. Estimated ammonium concentrations in July were low for all flow levels, which suggests either nitrogen inputs were low in the summer or nitrogen was available but uptake by primary consumers and bacterial processing were high. Seasonal patterns in the relationship between flow and nitrite/nitrate were not as dramatic as compared to ammonium, and in particular, low-flow events in July were associated with higher concentrations. This could suggest that ammonium concentrations at P8 are driving phytoplankton production at low flow during warmer months, and not nitrite/nitrate given the higher estimated concentrations in July at low flow. As such, these simple observations provide quantitative support of cause and effect mechanisms of nutrient impacts on potentially adverse environmental conditions as they relate to nutrient-related source controls upstream. Additional research could investigate these hypotheses to better describe mechanisms of change as a basis for more informed management.

The results for Suisun Bay provide additional descriptions of change in production as it relates to flow, grazing, and nitrogen ratios. In general, clam biomass was associated with a decrease in chl-*a* concentration, as shown by others (Alpine and Cloern 1992, Thompson et al. 2008). Our results also suggested that diatoms were the dominant genera

early in the time series, particularly in late summer, whereas the spring peak observed in later years represents a shift to an earlier seasonal maxima. This supports past research that showed a decrease in silica uptake by diatoms following invasion (Cloern 1996, Kimmerer 2005). A nontrivial portion of the DIN increase could be related to the decrease in a major 'sink', i.e., decreased DIN uptake by phytoplankton due to top down grazing pressure from *P. amurensis*. Flow effects on phytoplankton production have also changed over time. In the absence of benthic grazing prior to invasion, chl-*a* production was limited at low flow as less nutrients were exported from the Delta, stimulated as flow increases, and reduced at high flow as either nutrients or phytoplankton biomass are exported to the estuary (Fig. 7j). Recent years have shown a decrease in overall chlorophyll, with particularly low concentrations at low flow (high salinity). As such, chl-*a* production in early years is directly related to flow, whereas the relationship with flow in later years is indirect as increased flow reduces clam abundance and releases phytoplankton from benthic grazing pressure. These relationships have been suggested by others (Cloern et al. 1983, Alpine and Cloern 1992, Parchaso and Thompson 2002, Jassby 2008), although the precise mechanisms demonstrated by WRTDS provide additonal quantitative evidence of factors that drive water quality in the Delta.

4.2 Conclusions

As demonstrated by both case studies and the overall trends across all stations, water quality dynamics in the Delta are complex and driven by multiple factors that change through space and time. WRTDS models can facilitate descriptions of change by focusing on high-level forcing factors that explicitly account for annual, seasonal, and flow

effects on trend interpretations. We have demonstrated the potential for imprecise or inaccurate conclusions of trend tests that focus solely on observed data and emphasize that flow-normalized trends have more power to quantify change. The results from WRTDS are also consistent with described trends of nutrient loads from point sources (e.g., Sacramento WWTP increases and exports to Suisun Bay, Jassby 2008, Novick and Senn 2014), demonstrating that these changes are not unexpected. Consequently, we are not detracting from the potential implications of such increases. The important conclusion is that the physical/hydrological and biogeochemical factors that influence nutrient cycling and ambient concentrations in the Bay-Delta, and changes to those factors, are substantial enough that they can be comparable in magnitude to anthropogenic load increases or comparable to the effects of management actions to decrease nutrient levels. Therefore, methods that adjust for the effects of these factors are critical when studying long-term records to assess the impacts or effectiveness of load increases or management actions, respectively.

Combined with additional data, our results can support hypotheses that lead to a more comprehensive understanding of ecosystem dynamics. Additional factors to consider include the effects of large-scale climatic patterns, more detailed hydrologic descriptions, and additional ecological components that affect trophic interactions. For example, a more rigorous matching of flow time series with water quality observations at each station that considers varying source contributions over time could provide a more robust description of flow effects. Alternative methods could also be used to address a wider range of questions, particularly those with more generic structural forms that can explicitly include additional variables (e.g., generalized additive models, Beck and Murphy 2017). Overall, quantitative

interpretations of multiple factors can provide a more comprehensive understanding of relationships between nutrients and primary production, including adverse effects on ecosystem condition.

Acknowledgments

We thank the staff of the San Francisco Estuary Institute and the Delta Regional Monitoring Program. All data are from the California Department of Water Resources Environmental Monitoring Program. We thank Larry Harding, Raphael Mazor, Yongshan Wan, and Susan Elizabeth George for providing comments on an earlier draft. The authors declare no competing financial interest.

References

Alpine AE, Cloern JE. 1988. Phytoplankton growth rates in a light-limited environment, San Francisco Bay. Marine Ecology Progress Series, 44(2):167–173.

Alpine AE, Cloern JE. 1992. Trophic interactions and direct physical effects control phytoplankton biomass and production in an estuary. Limnology and Oceanography, 37(5):946–955.

ASC. 2017. Assessment of nutrient status and trends in the Delta in 2001-2016: Effects of drought on ambient concentrations and trends. Prepared by the Aquatic Science Center (ASC), T. Jabusch, P. Trowbridge, A. Wong, and M. Heberger for the Delta Regional Monitoring Program. Report v1.2.

Beck MW. 2017. WRTDStidal: Weighted Regression for Water Quality Evaluation in Tidal Waters. R package version 1.1.0.

Beck MW, Hagy III JD. 2015. Adaptation of a weighted regression approach to evaluate water quality trends in an estuary. Environmental Modelling and Assessment, 20(6):637–655.

Beck MW, Murphy RR. 2017. Numerical and qualitative contrasts of two statistical models for water quality change in tidal waters. Journal of the American Water Resources Association, 53(1):197–219.

Canuel EA, Lerberg EJ, Dickhut RM, Kuehl SA, Bianchi TS, Wakeham SG. 2009. Changes in sediment and organic carbon accumulation in a highly-disturbed ecosystem:

561 The Sacramento-San Joaquin River Delta (California, USA). Marine Pollution Bulletin,
562 59(4-7):154–163.

563 Cloern JE. 1996. Phytoplankton bloom dynamics in coastal ecosystems: A review with
564 some general lessons from sustained investigation of San Francisco Bay, California.
565 Review of Geophysics, 34(2):127–168.

566 Cloern JE. 2001. Our evolving conceptual model of the coastal eutrophication problem.
567 Marine Ecology Progress Series, 210:223–253.

568 Cloern JE. 2015. Life on the edge: California's estuaries. In: Mooney H, Zavaleta E,
569 editors, Ecosystems of California: A Source Book, pages 359–387. University of
570 California Press, California.

571 Cloern JE, Alpine AE, Cole BE, Wong RLJ, Arthur JF, Ball MD. 1983. River discharge
572 controls phytoplankton dynamics in the northern San Francisco Bay estuary. Estuarine,
573 Coastal and Shelf Science, 16(4):415–426.

574 Cloern JE, Jassby AD. 2010. Patterns and scales of phytoplankton variability in
575 estuarine-coastal ecosystems. Estuaries and Coasts, 33(2):230–241.

576 Cloern JE, Jassby AD. 2012. Drivers of change in estuarine-coastal ecosystems: Discoveries
577 from four decades of study in San Francisco Bay. Reviews of Geophysics, 50(4):1–33.

578 Cole BE, Cloern JE. 1984. Significance of biomass and light availability to phytoplankton
579 productivity in San Francisco Bay. Marine Ecology Progress Series, 17(1):15–24.

580 Cornwell JC, Glibert PM, Owens MS. 2014. Nutrient fluxes from sediments in the San
581 Francisco Bay Delta. Estuaries and Coasts, 37(5):1120–1133.

582 Dahm CN, Parker AE, Adelson AE, Christman MA, Bergamaschi BA. 2016. Nutrient
583 dynamics of the Delta: Effects on primary producers. San Francisco Estuary and
584 Watershed Science, 14(4):1–36.

585 Dugdale RC, Wilkerson FP, Hogue VE, Marchi A. 2007. The role of ammonium and
586 nitrate in spring bloom development in San Francisco Bay. Estuarine, Coastal, and Shelf
587 Science, 73:17–29.

588 Feyrer F, Herbold B, Matern SA, Moyle PB. 2003. Dietary shifts in a stressed fish
589 assemblage: Consequences of a bivalve invasion in the San Francisco Estuary.
590 Environmental Biology of Fishes, 67(3):277–288.

591 Glibert PM. 2010. Long-term changes in nutrient loading and stoichiometry and their
592 relationships with changes in the food web and dominant pelagic fish species in the San
593 Franciso Estuary, California. Reviews in Fisheries Science, 18(2):211–232.

594 Glibert PM, Dugdale RC, Wilkerson F, Parker AE, Alexander J, Antell E, Blaser S,
595 Johnson A, Lee J, Lee T, Murasko S, Strong S. 2014. Major - but rare - spring blooms in
596 san francisco bay delta, california, a result of long-term drought, increased residence

time, and altered nutrient loads and forms. Journal fo Experimental Marine Biology and Ecology, 460:8–18.

Harding LW, Gallegos CL, Perry ES, Miller WD, Adolf JE, Mallonee ME, Paerl HW. 2016. Long-term trends of nutrients and phytoplankton in Chesapeake Bay. Estuaries and Coasts, 39:664–681.

Hestir EL, Schoellhamer DH, Morgan-King T, Ustin SL. 2013. A step decrease in sediment concentration in a highly modifed tidal river delta following the 1983 El niño floods. Marine Geology, 345(1):304–313.

Hirsch RM, De Cicco L. 2014. User guide to Exploration and Graphics for RivEr Trends (EGRET) and dataRetrieval: R packages for hydrologic data. Technical Report Techniques and Methods book 4, ch. A10, US Geological Survey, Reston, Virginia. http://pubs.usgs.gov/tm/04/a10/.

Hirsch RM, Moyer DL, Archfield SA. 2010. Weighted regressions on time, discharge, and season (WRTDS), with an application to Chesapeake Bay river inputs. Journal of the American Water Resources Association, 46(5):857–880.

Hirsch RM, Slack JR, Smith RA. 1982. Techniques of trend analysis for monthly water quality data. Water Resources Research, 18:107–121.

IEP. 2013. IEP Bay-Delta Monitoring and Analysis Section, Discrete Water Quality Metadata. http://water.ca.gov/bdma/meta/discrete.cfm.

IEP. 2016. Dayflow: An estimate of daily average Delta outflow. Interagency Ecological Program for the San Francisco Estuary. http://www.water.ca.gov/dayflow/.

Jabusch T, Bresnahan P, Trowbridge P, Novick E, Wong A, Salomon M, Senn D. 2016. Summary and evaluation of Delta subregions for nutrient monitoring and assessment. Technical report, San Francisco Estuary Institute, Richmond, CA.

Jabusch T, Gilbreath AN. 2009. Summary of current water quality monitoring programs in the Delta. Technical report, San Francisco Estuary Institute, Richmond, CA.

Jassby AD. 2008. Phytoplankton in the Upper San Francisco Estuary: Recent biomass trends, their causes, and their trophic significance. San Francisco Estuary and Watershed Science, 6(1):1–24.

Jassby AD, Cloern JE. 2000. Organic matter sources and rehabilitations of the Sacramento-San Joaquin Delta (California, USA). Aquatic Conservation: Marine and Freshwater Ecosystems, 10:323–352.

Jassby AD, Cloern JE, Cole BE. 2002. Annual primary production: Patterns and mechanisms of change in a nutrient-rich tidal ecosystem. Limnology and Oceanography, 47(3):698–712.

Kimmerer W. 2005. Long-term changes in apparent uptake of silica in the San Francisco Estuary. Limnology and Oceanography, 50(3):793–798.

Kimmerer WJ, Parker AE, Lidstrom UE, Carpenter EJ. 2012. Short-term and interannual variability in primary production in the low-salinity zone of the San Francisco Estuary. Estuaries and Coasts, 35:913–929.

Kimmerer WJ, Thompson JK. 2014. Phytoplankton growth balanced by clam and zooplankton grazing and net transport into the low-salinity zone of the San Francisco Estuary. Estuaries and Coasts, 37:1202–1218.

Lehman PW. 1992. Environmental factors associated with long-term changes in chlorophyll concentration in the Sacramento-San Joaquin Delta and Suisun Bay, California. Estuaries, 15(3):335–348.

Lehman PW. 2000. The influence of climate on phytoplankton community biomass in San Francisco Bay Estuary. Limnology and Oceanography, 45(3):580–590.

Lehman PW, Boyer G, Hall C, Waller S, Gehrts K. 2005. Distribution and toxicity of a new colonial *Microcystis aeruginosa* bloom in the San Francisco Bay Estuary, California. Hydrobiologia, 541:87–99.

Lehman PW, Kendall C, Guerin MA, Young MB, Silva SR, Boyer GL, Teh SJ. 2015. Characterization of the *Microcystis* bloom and its nitrogen supply in San Francisco Estuary using stable isotopes. Estuaries and Coasts, 38(1):165–178.

Mac Nally R, Thompson JR, Kimmerer WJ, Feyrer F, Newman KB, Sih A, Bennett WA, Brown L, Fleishman E, Culberson SD, Castillo G. 2010. Analysis of pelagic species decline in the upper San Francisco Estuary using multivariate autoregressive modeling (MAR). Ecological Applications, 20(5):1417–1430.

Medalie L, Hirsch RM, Archfield SA. 2012. Use of flow-normalization to evaluate nutrient concentration and flux changes in Lake Champlain tributaries, 1990-2009. Journal of Great Lakes Research, 38(SI):58–67.

Millard SP. 2013. EnvStats: An R Package for Environmental Statistics. Springer, New York.

Nichols FH. 1985. Increased benthic grazing: An alternative explanation for low phytoplankton biomass in northern San Francisco Bay during the 1976-1977 drought. Estuarine, Coastal and Shelf Science, 21(3):379–388.

Novick E, Holleman R, Jabusch T, Sun J, Trowbridge P, Senn D, Guerin M, Kendall C, Young M, Peek S. 2015. Characterizing and quantifying nutrient sources, sinks and transformations in the Delta: synthesis, modeling, and recommendations for monitoring. Technical Report Contribution Number 785, San Francisco Estuary Institute, Richmond, CA.

668 Novick E, Senn D. 2014. External nutrient loads to San Francisco Bay. Technical Report
669 Contribution Number 704, San Francisco Estuary Institute, Richmond, CA.

670 Parchaso F, Thompson JK. 2002. Influence of hydrologic processes on reproduction of the
671 introduced bivalve *Potamocorbula amurensis* in northern San Francisco Bay, California.
672 Pacific Science, 56(3):329–345.

673 Pellerin BA, Bergamaschi BA, Gilliom RJ, Crawford CG, Saraceno JF, Frederick CP,
674 Downing BD, Murphy JC. 2014. Mississippi River nitrate loads from high frequency
675 sensor measurements and regression-based load estimation. Environmental Science and
676 Technology, 48:12612–12619.

677 RDCT (R Development Core Team). 2017. R: A language and environment for statistical
678 computing, v3.3.2. R Foundation for Statistical Computing, Vienna, Austria.
679 http://www.R-project.org.

680 Sakamoto M, Tanaka T. 1989. Phosphorus dynamics associated with phytoplankton
681 blooms in eutrophic Mikawa Bay, Japan. Marine Biology, 101(2):265–271.

682 Santos MJ, Khanna S, Hestir EL, Andrew ME. 2009. Use of hyperspectral remote sensing
683 to evaluate efficacy of aquatic plant management. Invasive Plant Science and
684 Management, 2(3):216–229.

685 Schoellhamer DH. 2011. Sudden clearing of estuarine waters upon crossing the threshold
686 from transport to supply regulation of sediment transport as an erodible sediment pool is
687 depleted: San francisco bay, 1999. Estuaries and Coasts, 34:885–899.

688 Schultz P, Urban NR. 2008. Effects of bacterial dynamics on organic matter decomposition
689 and nutrient release from sediments: A modeling study. Ecological Modelling,
690 210(1-2):1–14.

691 Sprague LA, Hirsch RM, Aulenbach BT. 2011. Nitrate in the Mississippi River and its
692 tributaries, 1980 to 2008: Are we making progress? Environmental Science and
693 Technology, 45(17):7209–7216.

694 Thompson JK, Koseff JR, Monismith SG, Lucas LV. 2008. Shallow water processes govern
695 system-wide phytoplankton bloom dynamics: A field study. Journal of Marine Systems,
696 74(1-2):153–166.

697 Thompson SE, Basu NB, Jr. JL, Aubeneau A, Rao PSC. 2011. Relative dominance of
698 hydrologic versus biogeochemical factors on solute export across impact gradients. Water
699 Resources Research, 47(10):W00J05.

700 Tobin J. 1958. Estimation of relationships for limited dependent variables. Econometrica,
701 26(1):24–36.

702 Wan Y, Wan L, Li Y, Doering P. 2017. Decadal and seasonal trends of nutrient
703 concentration and export from highly managed coastal catchments. Water Research,
704 115:180–194.

Wright SA, Schoellhamer DH. 2004. Trends in the sediment yield of the Sacramento River, California, 1957-2001. San Francisco Estuary and Watershed Science, 2(2):1–14.

Zhang Q, Harman CJ, Ball WP. 2016. An improved method for interpretation of riverine concentration-discharge relationships indicates long-term shifts in reservoir sediment trapping. Geophysical Research Letters, 43(10):215–224.

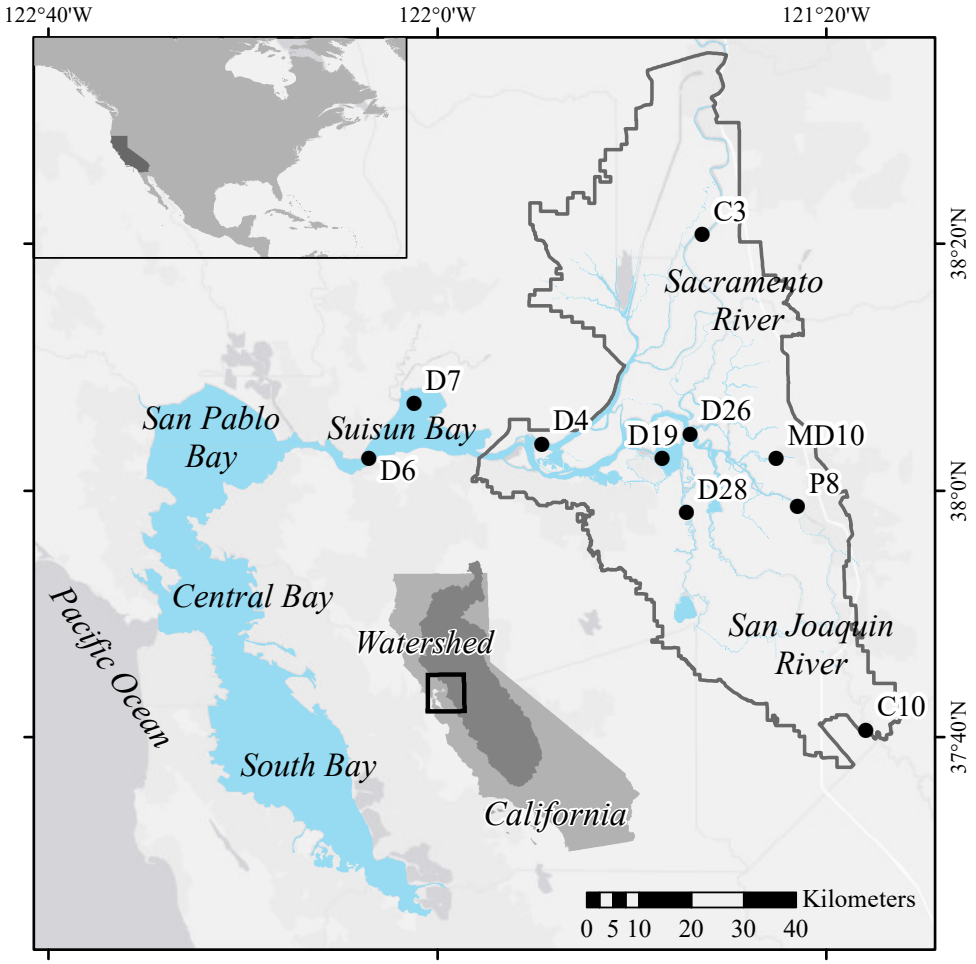

Fig. 1: The San Francisco Estuary and Delta region with monitoring stations used for analysis. The Delta drains the combined watersheds of the Sacramento and San Joaquin rivers (inset). The grey outline is the legal boundary of the Delta. All data were obtained from the Interagency Ecological Program website (http://water.ca.gov/bdma/meta/Discrete/data.cfm, IEP (2013)). See Table 1 for station descriptions.

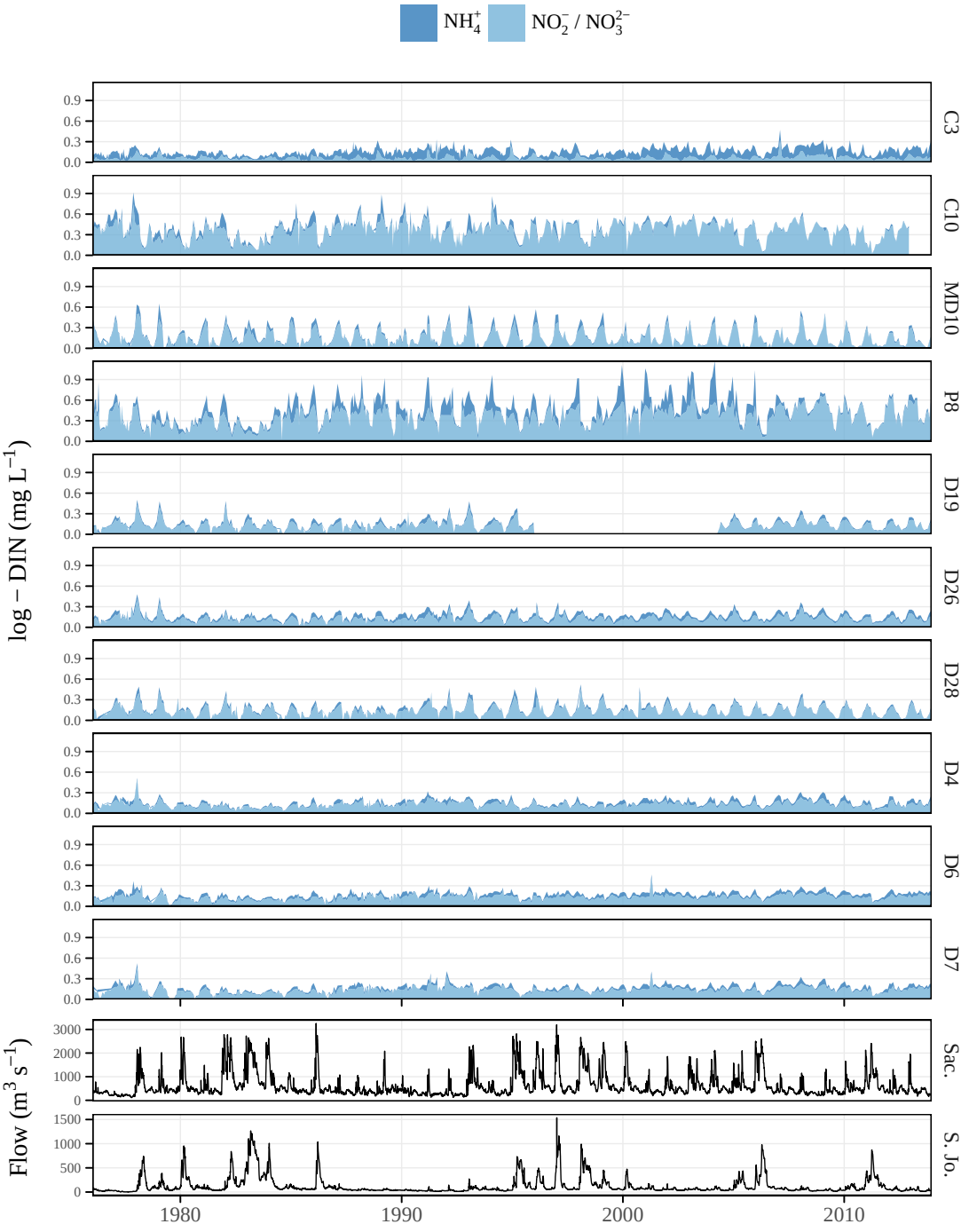

Fig. 2: Observed DIN (NH_4^+ + NO_2^-/NO_3^{2-}) from ten stations in the upper SFE Delta and flow from the Sacramento and San Joaquin rivers. Data were collected monthly and evaluated with WRTDS models using daily flow estimates from 1976 to 2013. Note different y-axis scales. See Fig. 1 for station locations.

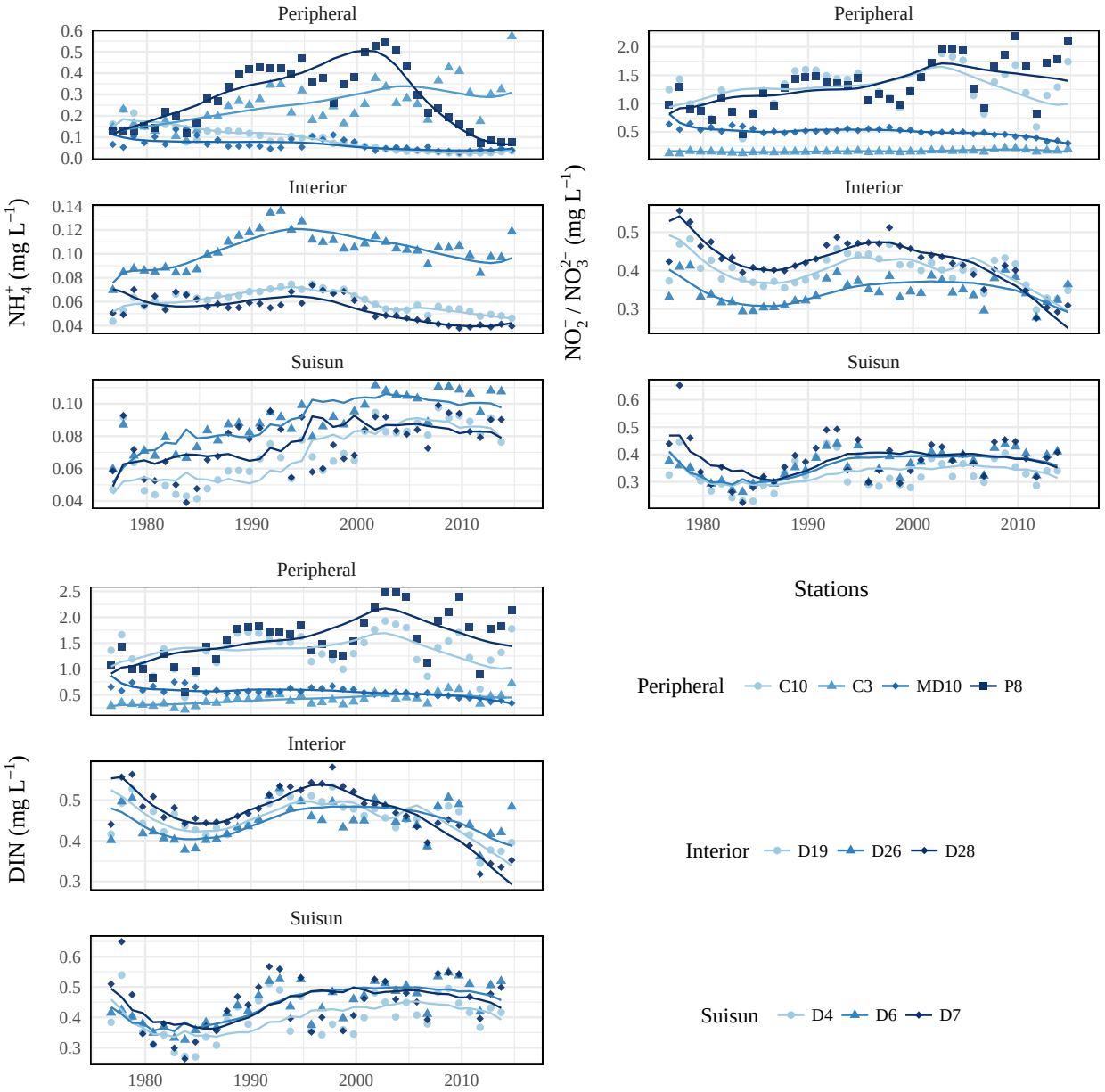

Fig. 3: Model results (points) and flow-normalized predictions (lines) for ten stations grouped by nitrogen analyte and geographic location in the Delta region (locations in Fig. 1). Results are annually-averaged for each water year from October to September.

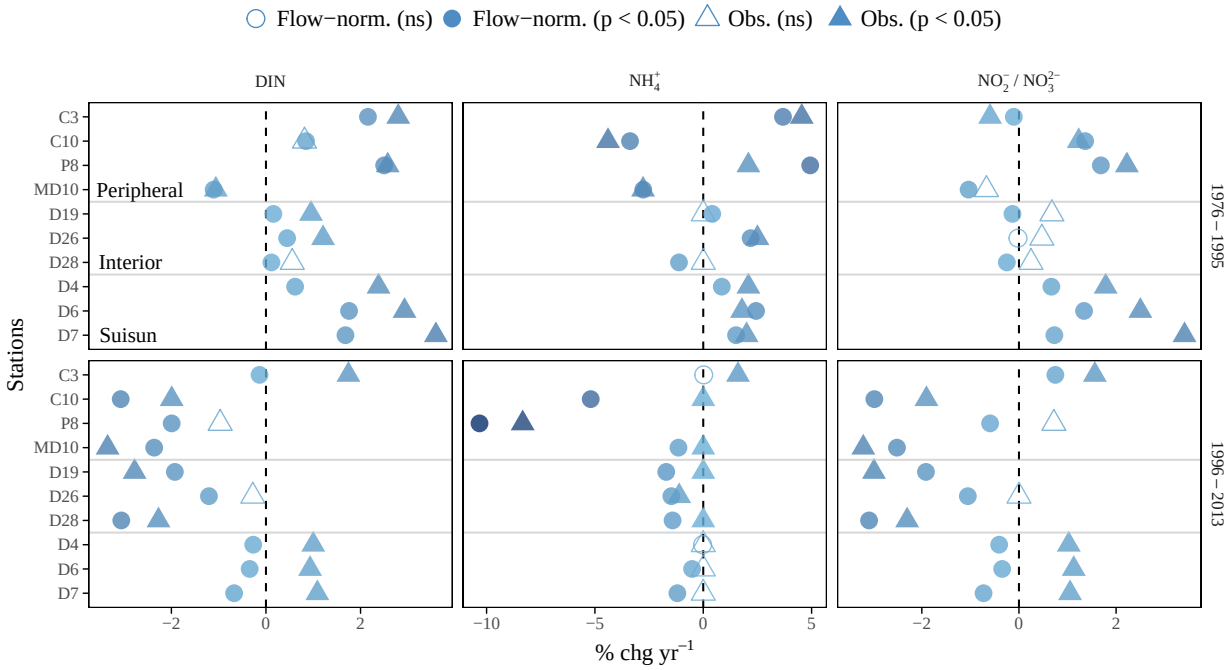

Fig. 4: Results from seasonal Kendall tests on observed data (triangles) and flow-normalized predictions (circles) from WRTDS for nitrogen forms. Results are shown as the percent change per year as the estimated Theil-Sen slope divided by the median for a given aggregation period (significance evaluated at $\alpha = 0.05$, based on τ). Trends are shown separately for different annual groupings from 1976 to 1995 (top) and 1996 to 2013 (bottom). See Figs. S1 and S2 for seasonal groupings.

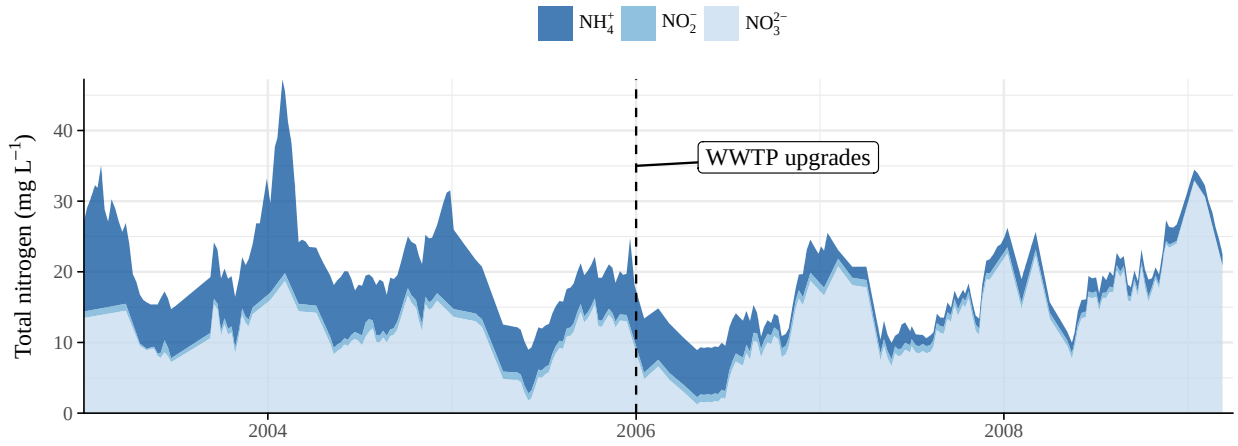

Fig. 5: Nitrogen concentration measurements (mg L^{-1}) from the City of Stockton Wastewater Treatment Plant, San Joaquin County. Wastewater discharge requirements were implemented in 2006 to convert ammonium to nitrate.

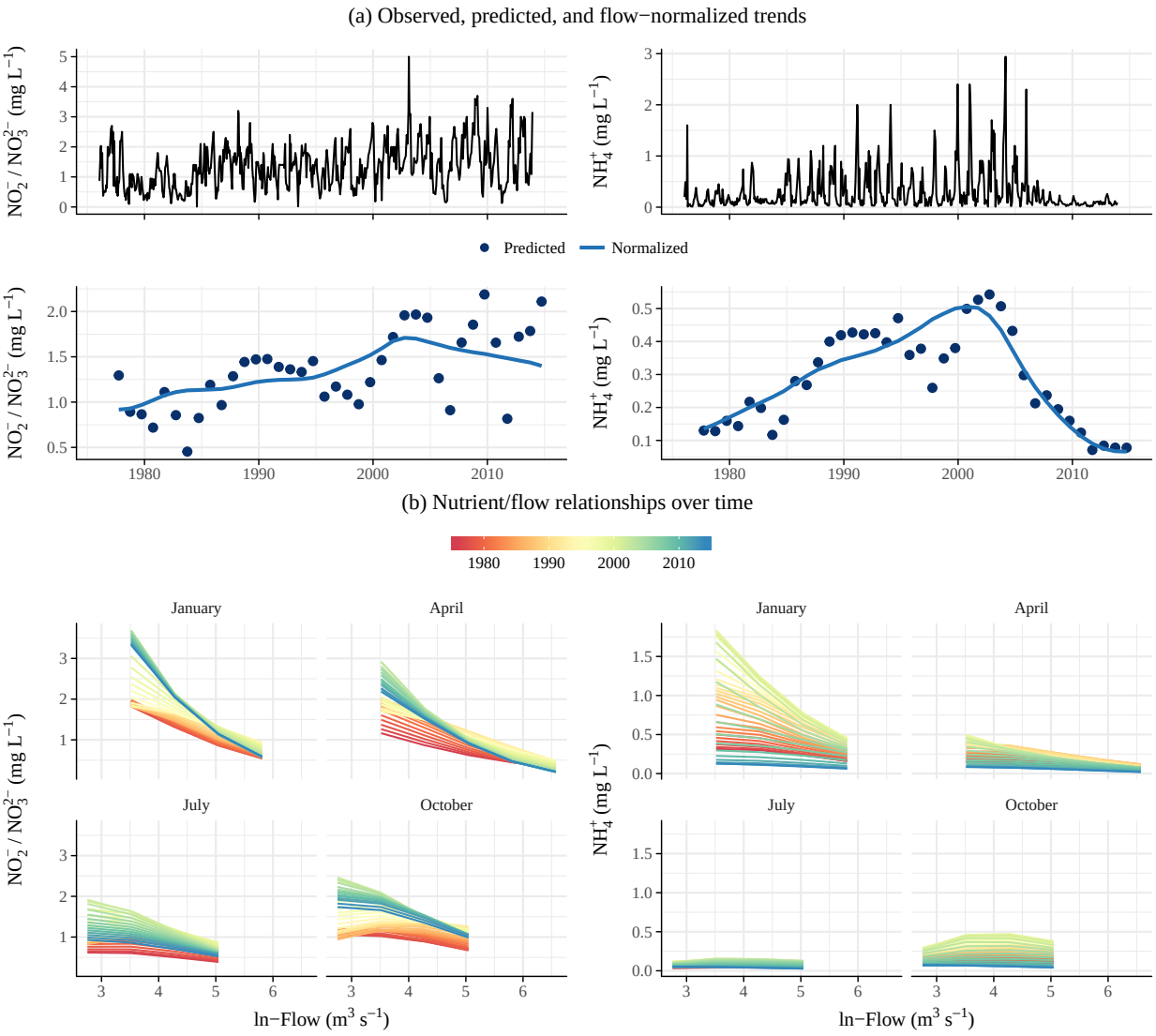

Fig. 6: Nitrogen trends at P8 as (a, top) observed, (a, bottom) predicted and flow-normalized estimates from WRTDS, and (b) relationships with flow over time from WRTDS. Nitrite/nitrate trends are on the left and ammonium trends are on the right. Wastewater treatment plant upgrades at the City of Stockton (San Joaquin County) were completed in 2006 (Fig. 5).

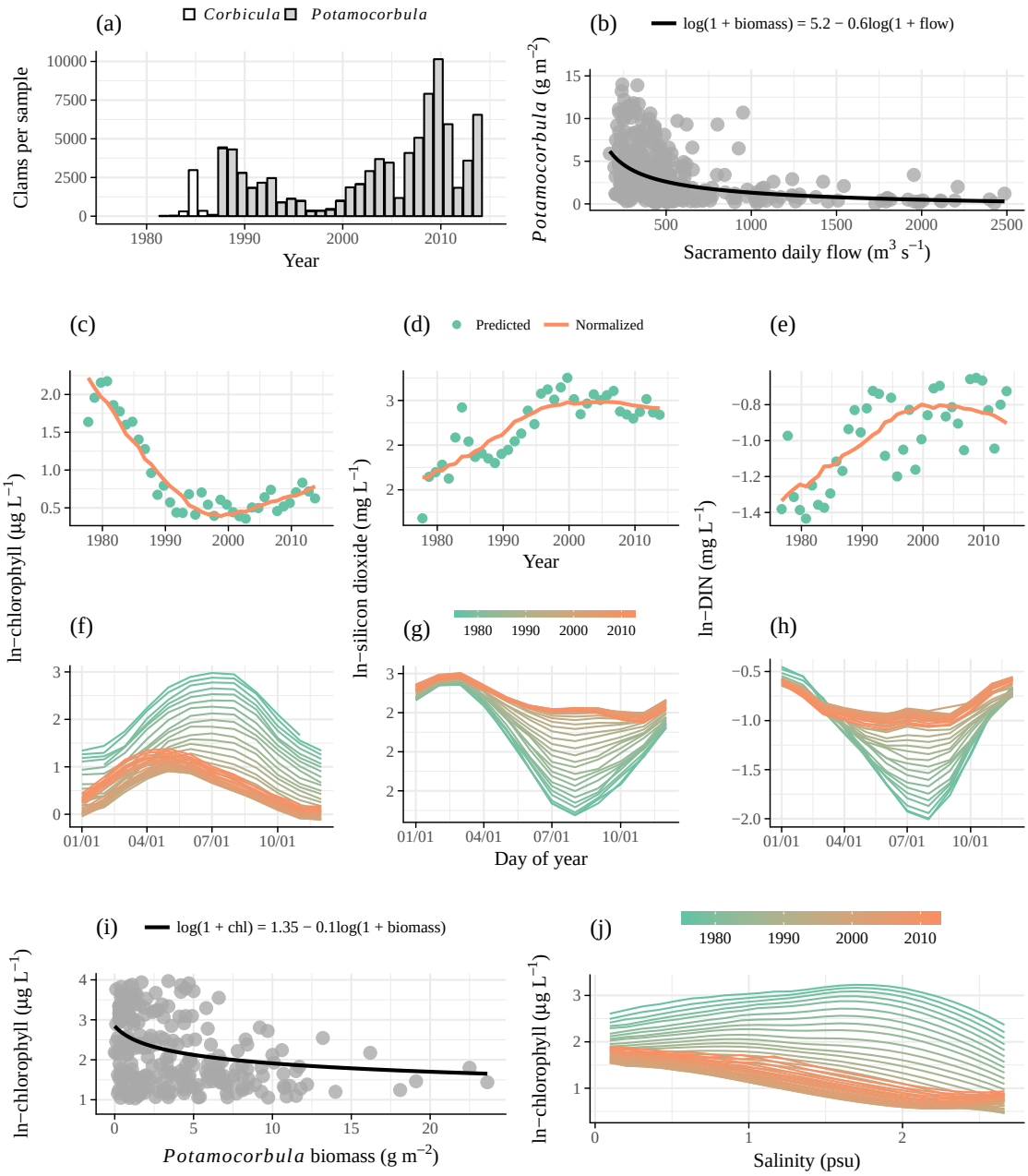

Fig. 7: Trends in clam abundance and chl-*a* concentration from 1976 to 2013 at station D7 in Suisun Bay. Invasion by *Potamocorbula amurensis* clams in the late 1980s and reduction of *Corbicula fluminea* was shown by changes in clam density (a, annual means), with biomass linked to salinity (b). A decrease in chl-*a* concentration was also observed by changes in annual (c) and seasonal trends (f) based on WRTDS results. Reductions in chl-*a* concentration were coincident with an increase in SiO_2 and DIN concentrations (d, e), with the greatest increases in August (g, h). A significant ($p < 0.001$) relationship between clam biomass and chl-*a* concentration is shown in subfigure (i). Flow relationships with chl-*a* concentration shown by WRTDS have also changed over time (j, observations from June).

Table 1: Monitoring stations in the upper San Francico Estuary used to evaluate nitrogen trends. Records from 1976 to 2013 were evaluated using the total observations (n) at each station. Median values (mg L^{-1}) are reported for the entire period of record.

Station			**DIN**		**NH_4^+**		**NO_2^-/NO_3^{2-}**	
	Lat	Lon	n	Med.	n	Med.	n	Med.
Peripheral								
C3	38.35	−121.55	569	0.36	569	0.22	571	0.13
C10	37.68	−121.27	539	1.44	539	0.04	558	1.40
MD10	38.04	−121.42	548	0.31	548	0.03	570	0.28
P8	37.98	−121.38	556	1.46	556	0.12	563	1.20
Interior								
D19	38.04	−121.61	433	0.35	435	0.04	462	0.31
D26	38.08	−121.57	556	0.38	556	0.09	565	0.29
D28	37.97	−121.57	529	0.38	535	0.03	555	0.33
Suisun								
D4	38.06	−121.82	546	0.38	546	0.05	565	0.32
D6	38.04	−122.12	534	0.45	534	0.08	562	0.35
D7	38.12	−122.04	535	0.44	535	0.06	561	0.36

Table 2: Summaries of flow-normalized trends in nitrogen forms for all stations and annual aggregations. Summaries are medians (mg L^{-1}) and percent change per year in parentheses (increasing in bold). Changes and significance estimates are based on seasonal Kendall tests of flow-normalized results within each time period. $^*p < 0.05$

Analyte/Station	**Annual**	
	1976-1995	1996-2013
DIN		
C10	1.3 (**0.8**)*	1.4 (-3.1)*
C3	0.3 (**2.2**)*	0.5 (-0.1)*
D19	0.4 (**0.2**)*	0.4 (-1.9)*
D26	0.4 (**0.4**)*	0.5 (-1.2)*
D28	0.4 (**0.1**)*	0.4 (-3.1)*
D4	0.3 (**0.6**)*	0.4 (-0.3)*
D6	0.4 (**1.8**)*	0.5 (-0.3)*
D7	0.4 (**1.7**)*	0.5 (-0.7)*
MD10	0.4 (-1.1)*	0.3 (-2.4)*
P8	1.3 (**2.5**)*	1.7 (-2)*
NH_4^+		
C10	0.1 (-3.4)*	0 (-5.2)*
C3	0.2 (**3.7**)*	0.3 (**0**)
D19	0 (**0.4**)*	0 (-1.7)*
D26	0.1 (**2.2**)*	0.1 (-1.5)*
D28	0 (-1.1)*	0 (-1.4)*
D4	0 (**0.9**)*	0.1 (**0**)
D6	0.1 (**2.4**)*	0.1 (-0.5)*
D7	0.1 (**1.5**)*	0.1 (-1.2)*
MD10	0.1 (-2.8)*	0 (-1.1)*
P8	0.2 (**4.9**)*	0.1 (-10.3)*
NO_2^-/NO_3^{2-}		
C10	1.2 (**1.4**)*	1.4 (-3)*
C3	0.1 (-0.1)*	0.2 (**0.7**)*
D19	0.4 (-0.1)*	0.4 (-1.9)*
D26	0.3 (**0**)	0.4 (-1.1)*
D28	0.4 (-0.2)*	0.4 (-3.1)*
D4	0.3 (**0.7**)*	0.3 (-0.4)*
D6	0.3 (**1.3**)*	0.4 (-0.3)*
D7	0.4 (**0.7**)*	0.4 (-0.7)*
MD10	0.4 (-1)*	0.3 (-2.5)*
P8	1.2 (**1.7**)*	1.5 (-0.6)*

Table 3: Summaries of flow-normalized trends in nitrite/nitrate and ammonium (mg L^{-1}) concentrations before and after WWTP upgrades upstream of station P8. Upgrades were completed in 2006 at the City of Stockton WWTP (San Joaquin County, Fig. 5). Summaries are medians and percent change per year in parentheses (increasing in bold). Changes and significance estimates are based on seasonal Kendall tests of flow-normalized results within each time period. Increasing values are in bold-italics. Months for each season are Spring: MAM, Summer: JJA, Fall: SON, Winter: DJF. $^*p < 0.05$

Period	$\mathbf{NO_2^-/NO_3^{2-}}$		$\mathbf{NH_4^+}$	
	Median	% change	Median	% change
Annual				
1976-2006	1.3	**2***	0.2	**2.8***
2007-2013	1.4	-1.9*	0.1	-16.6*
Seasonal, pre				
Spring	1.2	**1.6***	0.2	**1.4***
Summer	1	**2.4***	0.1	**3.3***
Fall	1.3	**2.2***	0.2	**4.9***
Winter	1.5	**2.1***	0.7	**4.8***
Seasonal, post				
Spring	1.3	-1.6*	0.1	-16.2*
Summer	0.9	-4.3*	0.1	-15.7*
Fall	1.5	-1.7*	0.1	-19.3*
Winter	2.2	-0.8*	0.2	-26.7*

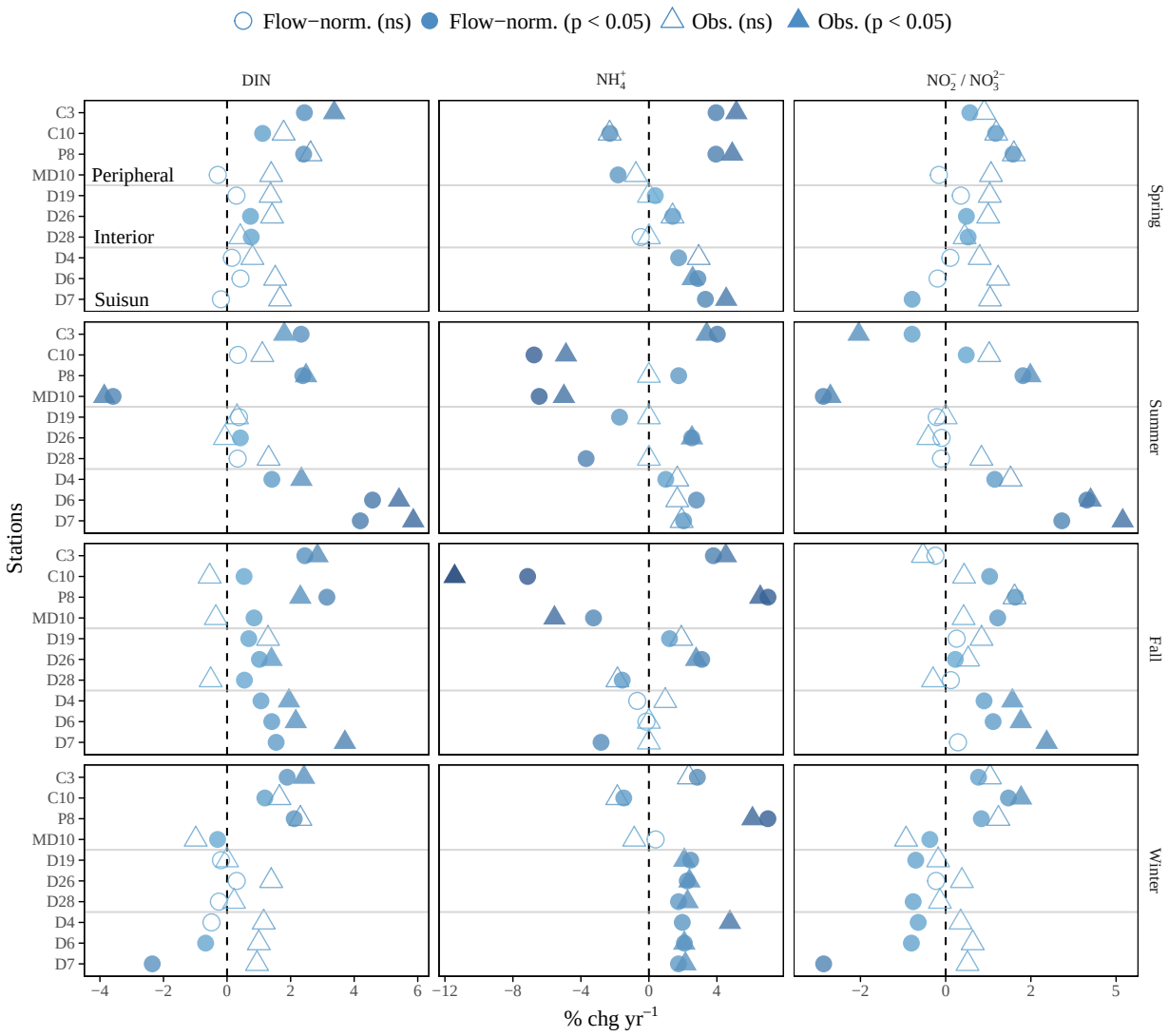

Fig. S1: Results from seasonal Kendall tests on observed data (triangles) and flow-normalized predictions (circles) from WRTDS for nitrogen forms. Results are shown as the percent change per year as the estimated Theil-Sen slope divided by the median for a given aggregation period (significance evaluated at $\alpha = 0.05$, based on τ). Trends are shown separately for different seasonal groupings from 1976-1995. Months for each season are Spring: MAM, Summer: JJA, Fall: SON, Winter: DJF. See Fig. 4 for annual comparisons.

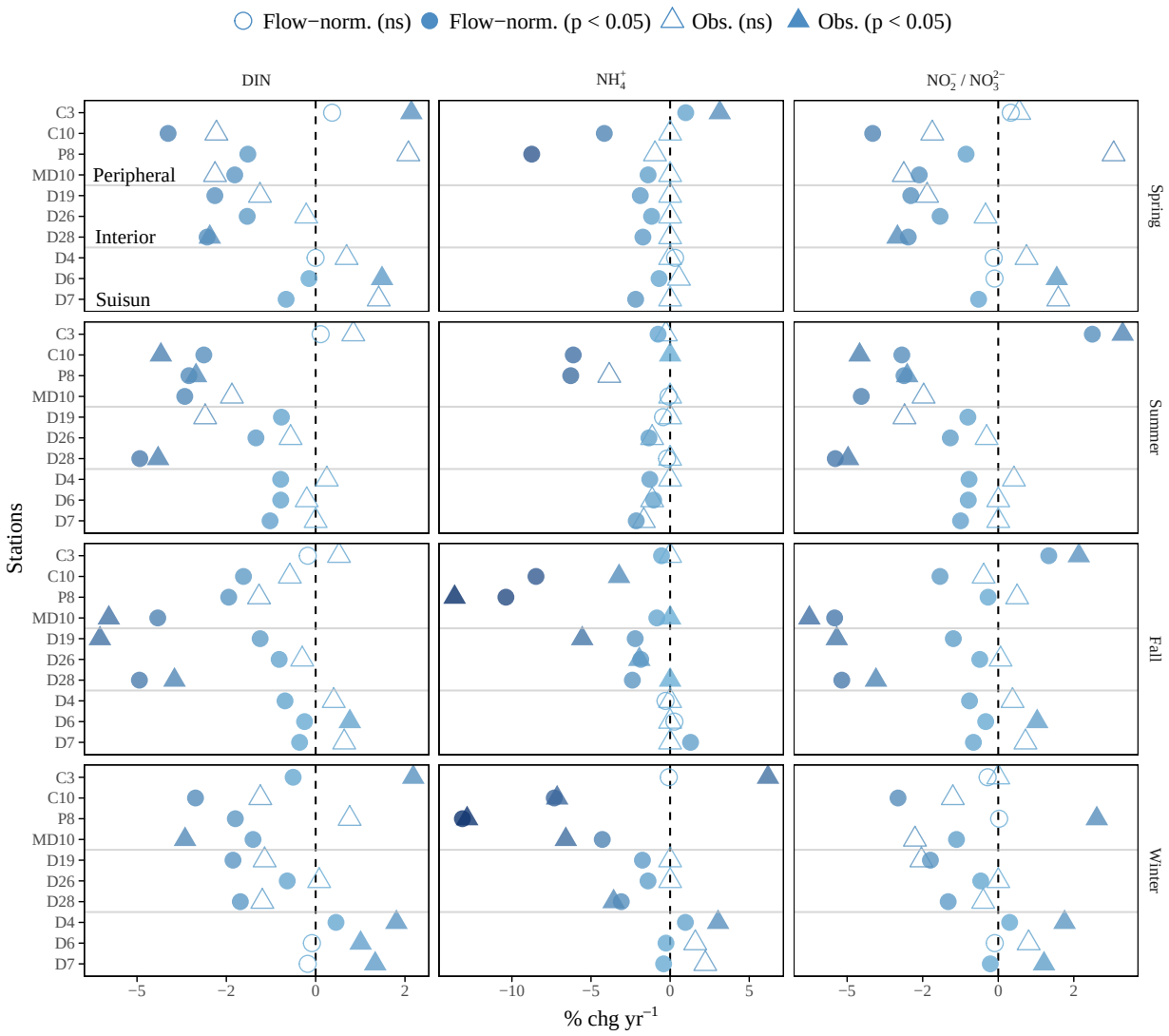

Fig. S2: Results from seasonal Kendall tests on observed data (triangles) and flow-normalized predictions (circles) from WRTDS for nitrogen forms. Results are shown as the percent change per year as the estimated Theil-Sen slope divided by the median for a given aggregation period (significance evaluated at $\alpha = 0.05$, based on τ). Trends are shown separately for different seasonal groupings from 1996-2013. Months for each season are Spring: MAM, Summer: JJA, Fall: SON, Winter: DJF. See Fig. 4 for annual comparisons.

Table S1: Summaries of flow-normalized trends in nitrogen forms for all stations and seasonal aggregations from 1976-1995. Summaries are medians (mg L^{-1}) and percent change per year in parentheses (increasing in bold). Changes and significance estimates are based on seasonal Kendall tests of flow-normalized results within each time period. Months for each season are Spring: MAM, Summer: JJA, Fall: SON, Winter: DJF. $^*p < 0.05$

Analyte/Station	**Seasonal, 1976-1995**			
	Spring	Summer	Fall	Winter
DIN				
C10	1.2 (**1.1**)*	1.2 (**0.3**)	1.3 (**0.5**)*	1.7 (**1.2**)*
C3	0.3 (**2.4**)*	0.3 (**2.3**)*	0.4 (**2.4**)*	0.4 (**1.9**)*
D19	0.5 (**0.3**)	0.2 (**0.4**)	0.3 (**0.7**)*	0.7 (-0.2)
D26	0.4 (**0.7**)*	0.3 (**0.4**)*	0.4 (**1**)*	0.6 (**0.3**)
D28	0.5 (**0.8**)*	0.2 (**0.3**)	0.3 (**0.5**)*	0.8 (-0.3)
D4	0.4 (**0.2**)	0.3 (**1.4**)*	0.3 (**1.1**)*	0.5 (-0.5)
D6	0.4 (**0.4**)	0.3 (**4.6**)*	0.4 (**1.4**)*	0.5 (-0.7)*
D7	0.4 (-0.2)	0.3 (**4.2**)*	0.4 (**1.5**)*	0.6 (-2.4)*
MD10	0.6 (-0.3)	0.2 (-3.6)*	0.3 (**0.8**)*	1.3 (-0.3)*
P8	1.3 (**2.4**)*	0.9 (**2.4**)*	1.3 (**3.1**)*	1.9 (**2.1**)*
NH_4^+				
C10	0.1 (-2.3)*	0 (-6.8)*	0.1 (-7.1)*	0.3 (-1.5)*
C3	0.2 (**3.9**)*	0.2 (**4**)*	0.3 (**3.8**)*	0.2 (**2.9**)*
D19	0.1 (**0.4**)*	0 (-1.7)*	0 (**1.2**)*	0.1 (**2.5**)*
D26	0.1 (**1.4**)*	0.1 (**2.5**)*	0.1 (**3.1**)*	0.1 (**2.3**)*
D28	0.1 (-0.5)	0 (-3.7)*	0 (-1.6)*	0.1 (**1.7**)*
D4	0.1 (**1.7**)*	0 (**1**)*	0 (-0.7)	0.1 (**2**)*
D6	0.1 (**2.9**)*	0.1 (**2.8**)*	0.1 (-0.1)	0.1 (**2.1**)*
D7	0.1 (**3.3**)*	0 (**2**)*	0.1 (-2.8)*	0.1 (**1.7**)*
MD10	0.1 (-1.8)*	0 (-6.5)*	0 (-3.3)*	0.2 (**0.4**)
P8	0.2 (**3.9**)*	0.1 (**1.8**)*	0.2 (**7**)*	0.6 (**7**)*
NO_2^-/NO_3^{2-}				
C10	1.1 (**1.5**)*	1.2 (**0.6**)*	1.2 (**1.3**)*	1.5 (**1.8**)*
C3	0.2 (**0.7**)*	0.1 (-1)*	0.1 (-0.3)	0.2 (**1**)*
D19	0.4 (**0.4**)	0.2 (-0.3)	0.3 (**0.3**)	0.6 (-0.9)*
D26	0.4 (**0.6**)*	0.2 (-0.1)	0.3 (**0.3**)*	0.5 (-0.3)
D28	0.5 (**0.7**)*	0.2 (-0.1)	0.3 (**0.2**)	0.7 (-1)*
D4	0.3 (**0.1**)	0.3 (**1.4**)*	0.3 (**1.1**)*	0.4 (-0.8)*
D6	0.4 (-0.2)	0.3 (**4.1**)*	0.3 (**1.4**)*	0.4 (-1)*
D7	0.4 (-1)*	0.3 (**3.4**)*	0.4 (**0.4**)	0.4 (-3.6)*
MD10	0.5 (-0.2)	0.2 (-3.6)*	0.2 (**1.5**)*	1.2 (-0.5)*
P8	1.2 (**2**)*	0.9 (**2.3**)*	1.1 (**2**)*	1.4 (**1**)*

Table S2: Summaries of flow-normalized trends in nitrogen forms for all stations and seasonal aggregations from 1996-2013. Summaries are medians (mg L^{-1}) and percent change per year in parentheses (increasing in bold). Changes and significance estimates are based on seasonal Kendall tests of flow-normalized results within each time period. Months for each season are Spring: MAM, Summer: JJA, Fall: SON, Winter: DJF. $^*p < 0.05$

Analyte/Station	**Seasonal, 1996-2013**			
	Spring	Summer	Fall	Winter
DIN				
C10	1.1 (-4.1)*	1.3 (-3.1)*	1.6 (-2)*	1.7 (-3.4)*
C3	0.5 (**0.5**)	0.4 (**0.1**)	0.6 (-0.2)	0.5 (-0.6)*
D19	0.5 (-2.8)*	0.2 (-1)*	0.3 (-1.6)*	0.7 (-2.3)*
D26	0.5 (-1.9)*	0.3 (-1.7)*	0.4 (-1)*	0.6 (-0.8)*
D28	0.5 (-3)*	0.2 (-4.9)*	0.2 (-4.9)*	0.7 (-2.1)*
D4	0.4 (**0**)	0.4 (-1)*	0.4 (-0.9)*	0.5 (**0.6**)*
D6	0.5 (-0.2)*	0.5 (-1)*	0.5 (-0.3)*	0.5 (-0.1)
D7	0.5 (-0.8)*	0.4 (-1.3)*	0.4 (-0.4)*	0.6 (-0.2)
MD10	0.4 (-2.3)*	0.2 (-3.7)*	0.2 (-4.4)*	1 (-1.8)*
P8	1.5 (-1.9)*	1.2 (-3.5)*	1.8 (-2.4)*	2.7 (-2.2)*
$\mathbf{NH_4^+}$				
C10	0 (-4.2)*	0 (-6.1)*	0 (-8.5)*	0.1 (-7.3)*
C3	0.3 (**1**)*	0.3 (-0.8)*	0.4 (-0.5)*	0.2 (-0.1)
D19	0 (-1.9)*	0 (-0.4)	0 (-2.2)*	0.1 (-1.8)*
D26	0.1 (-1.2)*	0.1 (-1.3)*	0.1 (-1.9)*	0.1 (-1.4)*
D28	0 (-1.7)*	0 (-0.2)	0 (-2.4)*	0.1 (-3.1)*
D4	0.1 (**0.3**)	0 (-1.3)*	0.1 (-0.3)	0.1 (**1**)*
D6	0.1 (-0.7)*	0.1 (-1)*	0.1 (**0.3**)	0.1 (-0.3)*
D7	0.1 (-2.2)*	0 (-2.1)*	0.1 (**1.3**)*	0.1 (-0.4)*
MD10	0 (-1.4)*	0 (-0.1)	0 (-0.8)*	0.1 (-4.3)*
P8	0.2 (-8.7)*	0.1 (-6.3)*	0.2 (-10.4)*	0.5 (-13.1)*
$\mathbf{NO_2^-/NO_3^{2-}}$				
C10	1.1 (-4.2)*	1.2 (-3.2)*	1.6 (-1.9)*	1.6 (-3.3)*
C3	0.2 (**0.4**)	0.1 (**3.1**)*	0.2 (**1.7**)*	0.2 (-0.4)
D19	0.4 (-2.9)*	0.2 (-1)*	0.3 (-1.5)*	0.6 (-2.2)*
D26	0.4 (-1.9)*	0.2 (-1.6)*	0.3 (-0.6)*	0.5 (-0.6)*
D28	0.5 (-3)*	0.2 (-5.4)*	0.2 (-5.2)*	0.7 (-1.7)*
D4	0.3 (-0.1)	0.3 (-1)*	0.3 (-1)*	0.4 (**0.4**)*
D6	0.4 (-0.1)	0.4 (-1)*	0.4 (-0.4)*	0.4 (-0.1)
D7	0.4 (-0.6)*	0.4 (-1.2)*	0.4 (-0.8)*	0.4 (-0.3)*
MD10	0.4 (-2.6)*	0.1 (-4.5)*	0.2 (-5.4)*	1 (-1.4)*
P8	1.3 (-1.1)*	1.1 (-3.1)*	1.6 (-0.3)*	2.2 (**0**)